A Note on Computational Rotor Dynamics

W. J. Chen
Centrifugal Compressor Division,
Ingersoll-Rand Company,
Mayfield, Kentucky

Concise equations for improvements in computational efficiency on dynamics of rotor systems are presented. Two coordinate ordering methods are introduced in the element equations of motion. One is in the real domain and the other is in the complex domain. The two coordinate ordering algorithms lead to compact element matrices. A station numbering technique is also proposed for the system equations during the assembly process. The proposed numbering technique can minimize the matrix bandwidth, the memory storage and can increase the computational efficiency. Numerical examples are presented to demonstrate the benefit of the proposed algorithms.

Introduction

Since 1970, the finite element method has been used extensively in the analysis of rotordynamic systems. Ease of implementation, expandability, adaptability, and access to a large library of well-developed mathematical functions are several features that make the finite element method an attractive and indispensable tool in the field of rotor dynamics. For a complicated rotor-bearing-foundation system, the system matrices in the governing equations of motion are generally large and sparse. Consequently, the computer memory storage requirements and computation time may also be large. Nelson (1985) proposed that a complex form of the finite element equations could be used to reduce the array size and also increase computational efficiency. The array sizes in his approach are reduced by a factor of two and the resulting matrices are complex Hermitian. Shiau and Hwang (1989) and Nelson and Chen (1993) have proposed a modeling procedure using assumed modes to reduce the order of the system matrices. The resulting accuracy and computational effectiveness depend upon the type and number of modes used in the reduction process. The problem of computational storage, however, remains the same.

This paper presents more concise forms for the formulation of the equations of motion. The proposed method utilizes coordinate and station numbering schemes at both the element and system levels to reduce the computer memory storage requirements and improve computational efficiency without reducing accuracy. Savings in computer time can accelerate design iterations and shorten the product development cycle. The reordering schemes are implemented within a computer code and the coordinate order, selected by the analyst, is preserved in the final results. Two examples are presented to illustrate the savings in computational efforts.

Element Equation

The motion of a finite shaft element, as shown in Fig. 1, is described by eight end-point displacements including two translational displacements in the (X, Y) directions and two rotational displacements about the (X, Y) axes at each end point. The shaft element is assumed to be isotropic and symmetric about the axis of rotation (Z). Conventionally, the time dependent end-point displacements are arranged in the following form (Rouch and Kao, 1979; Nelson, 1980; Ehrich, 1992):

$$\mathbf{q}^e = (\mathbf{q}_1, \mathbf{q}_2)^T = (x_1, y_1, \theta_{x1}, \theta_{y1}, x_2, y_2, \theta_{x2}, \theta_{y2})^T \quad (1)$$

where $\mathbf{q}_1$ and $\mathbf{q}_2$ are the left and right end displacement vectors, respectively. The eight degree-of-freedom element equation of motion becomes:

$$\mathbf{M}^e\ddot{\mathbf{q}}^e + \mathbf{G}^e\dot{\mathbf{q}}^e + \mathbf{K}^e\mathbf{q}^e = \mathbf{Q}^e \quad (2)$$

The (8×8) element mass $(\mathbf{M}^e)$ and stiffness $(\mathbf{K}^e)$ matrices are symmetric and the gyroscopic matrix $(\mathbf{G}^e)$ is skew-symmetric. Details for these matrices are listed in Nelson (1980) and are not repeated here. Due to the symmetry and skew-symmetry properties of the system matrices, 36 real coefficients are required to be stored for each element matrix. A full matrix manipulation is required when the equations are written in this form.

More compact element and system equations of motion in a complex form were presented by Nelson (1985). The complex end-point displacement vector is defined as

$$\hat{\mathbf{q}}^e = \begin{Bmatrix} x_1 + jy_1 \\ \theta_{x1} + j\theta_{y1} \\ x_2 + jy_2 \\ \theta_{x2} + j\theta_{y2} \end{Bmatrix}, \quad (3)$$

and the element equation of motion is written in the complex form:

$$\hat{\mathbf{M}}^e\ddot{\hat{\mathbf{q}}}^e + \hat{\mathbf{G}}^e\dot{\hat{\mathbf{q}}}^e + \hat{\mathbf{K}}^e\hat{\mathbf{q}}^e = \hat{\mathbf{Q}}^e \quad (4)$$

The size of the element matrices in Eq. (4) is reduced by a factor of two resulting in a more compact form. Computational efficiency is increased by the use of complex matrix solvers and because less index manipulation is required. Unfortunately, the elements of the matrices are complex, although the matrices are Hermitian. This complex coordinate approach was also adopted by Genta (1988) in the study of unsymmetrical rotors.

Ruhl and Booker (1972) presented a finite element model in rotor systems with rotor motions in two lateral planes. The gyroscopic moments were neglected and the two planes of motion were decoupled. Following the work of Nelson (1980), Childs and Graviss (1982) utilized a coordinate reordering scheme to partition the motion into two planes in the calculation of undamped critical speeds. This reordering procedure permits the critical speeds to be determined directly using symmetric matrix manipulations. For isotropic rotor systems, only one plane of motion is required for the calculation of undamped critical speeds. Hashish and Sankar (1984) utilized this ordering procedure in the study of rotor response under stochastic loading conditions. To order the displacements in the XZ and YZ planes, the displacement vector is arranged in the following form:

Contributed by the Technical Committee on Vibration and Sound for publication in the JOURNAL OF VIBRATION AND ACOUSTICS. Manuscript received Dec. 1994. Associate Technical Editor: S. Noah.

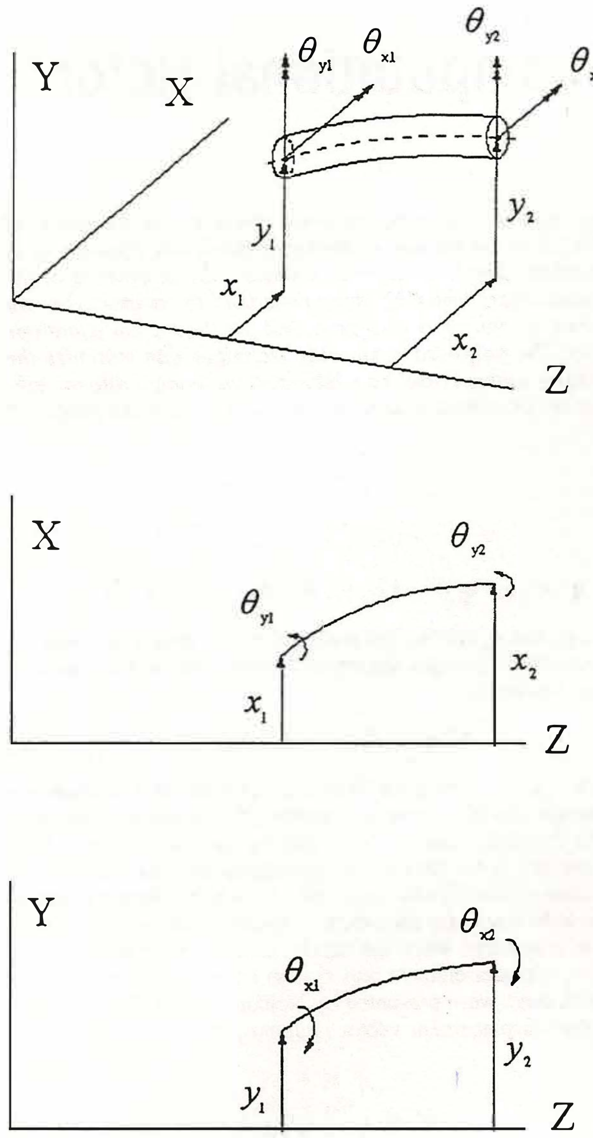

Fig. 1 A typical shaft element and coordinates

$$\mathbf{q}^e = (\mathbf{q}_{XZ}, \mathbf{q}_{YZ})^T = (x_1, \theta_{y1}, x_2, \theta_{y2}, y_1, -\theta_{x1}, y_2, -\theta_{x2})^T \quad (5)$$

where $\mathbf{q}_{XZ}$ and $\mathbf{q}_{YZ}$ are the displacement vectors in the XZ and YZ planes, respectively. Negative signs are added in the rotational displacements of the YZ plane so that the static beam element matrices are identical in both planes. The element equations of motion are then of the form:

$$\begin{bmatrix} \mathbf{M}^e_{XZ} & \mathbf{0} \\ \mathbf{0} & \mathbf{M}^e_{YZ} \end{bmatrix} \begin{Bmatrix} \ddot{\mathbf{q}}_{XZ} \\ \ddot{\mathbf{q}}_{YZ} \end{Bmatrix} + \begin{bmatrix} \mathbf{0} & -\mathbf{G}^e_{XY} \\ \mathbf{G}^e_{XY} & \mathbf{0} \end{bmatrix} \begin{Bmatrix} \dot{\mathbf{q}}_{XZ} \\ \dot{\mathbf{q}}_{YZ} \end{Bmatrix} + \begin{bmatrix} \mathbf{K}^e_{XZ} & \mathbf{0} \\ \mathbf{0} & \mathbf{K}^e_{YZ} \end{bmatrix} \begin{Bmatrix} \mathbf{q}_{XZ} \\ \mathbf{q}_{YZ} \end{Bmatrix} = \begin{Bmatrix} \mathbf{Q}_{XZ} \\ \mathbf{Q}_{YZ} \end{Bmatrix} \quad (6)$$

This equation shows that the two planes of motion are coupled only through the gyroscopic effect. Again, the (8×8) element mass and stiffness matrices are symmetric and the gyroscopic matrix is skew-symmetric. Since the shaft element is isotropic, the mass and stiffness matrices in both planes are identical and the sub-matrix of the gyroscopic matrix becomes symmetric, i.e.,

$$\mathbf{M}^e_{XZ} = \mathbf{M}^e_{YZ}, \quad \mathbf{K}^e_{XZ} = \mathbf{K}^e_{YZ}, \quad \mathbf{G}^e_{XY} = \mathbf{G}^{eT}_{XY} \quad (7)$$

Thus, only 10 real coefficients are required to be stored for each element matrix.

A more compact form of Eq. (6) is proposed in this paper to further reduce the Hermitian matrices presented by Nelson (1985) to real symmetric matrices. This is accomplished by arranging the displacements of one plane in the real domain and the displacements of the other plane in the imaginary domain. The complex displacement vector is defined as

$$\hat{\mathbf{q}}^e = \mathbf{q}_{XZ} + j\mathbf{q}_{YZ} = \begin{Bmatrix} x_1 \\ \theta_{y1} \\ x_2 \\ \theta_{y2} \end{Bmatrix} + j \begin{Bmatrix} y_1 \\ -\theta_{x1} \\ y_2 \\ -\theta_{x2} \end{Bmatrix} = \begin{Bmatrix} x_1 + jy_1 \\ \theta_{y1} - j\theta_{x1} \\ x_2 + jy_2 \\ \theta_{y2} - j\theta_{x2} \end{Bmatrix}, \quad (8)$$

and the related complex equations of motion, from Eq. (6), are

$$\mathbf{M}^e_{XZ}\ddot{\hat{\mathbf{q}}}^e + j\mathbf{G}^e_{XY}\dot{\hat{\mathbf{q}}}^e + \mathbf{K}^e_{XZ}\hat{\mathbf{q}}^e = \hat{\mathbf{Q}}^e \quad (9)$$

All of the element matrices in Eq. (9) are real and symmetric and the gyroscopic matrix is directly obtained from the rotatory mass matrix. The coefficients for the matrices in Eq. (9) are listed in the Appendix.

System Equation

The conventional station numbering scheme and assembly process is illustrated in Ehrich (1992) using a dual-shaft system, shown in Fig. 2. This system consists of two flexible rotors interconnected by an intershaft bearing. Each shaft includes two rigid disks. The rotor system is supported by three bearings with flexible housings. A schematic of the system with both the conventional and proposed station numbers is shown in Fig. 3. Numbers outside the parentheses represent the conventional station number ordering scheme and numbers inside the paren-

Nomenclature

A = cross-sectional area
$\mathbf{C}$ = damping matrix
EI = bending modulus
G = shear modulus
$\mathbf{G}$ = gyroscopic matrix
$j = \sqrt{-1}$
κ = shape factor
$\mathbf{K}$ = stiffness matrix
l = element length
$\mathbf{M}$ = mass/inertia matrix
m, n = coefficients
$\mathbf{Q}$ = force vector
$\mathbf{q}$ = displacement vector
(x, y) = translational displacements
(θ_x, θ_y) = rotational displacement
Ω = rotor speed
ρA = unit mass
ρI = moment of inertia
$\Phi = 12EI/\kappa GAl^2$, transverse shear effect

Superscripts

e = element

Subscripts

1, 2 = left, right end of the element
T, R = translation, rotation
XZ = X-Z plane
YZ = Y-Z plane

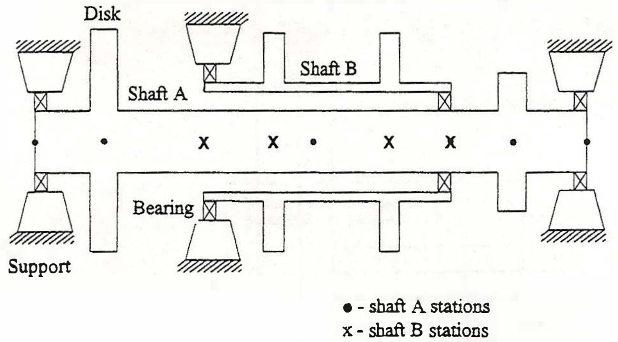

Fig. 2 Dual-shaft system

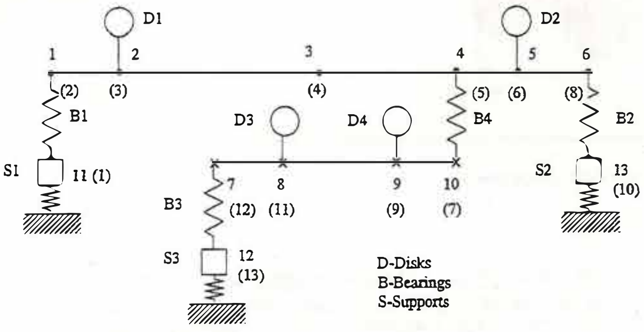

Fig. 3 System schematic and station numbers

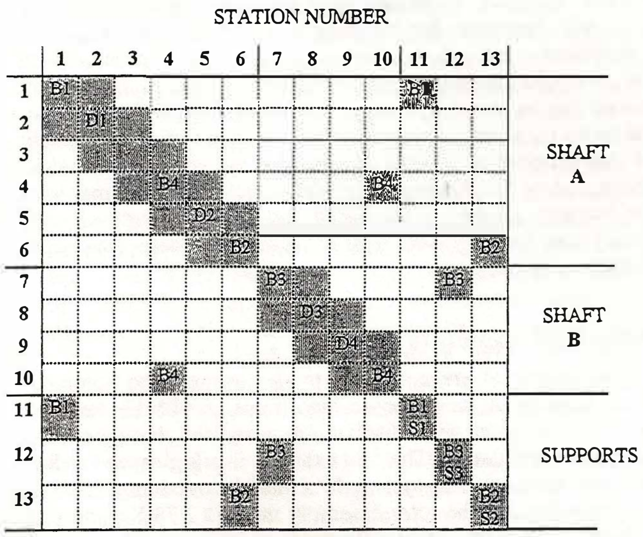

Fig. 4 Conventional system matrices

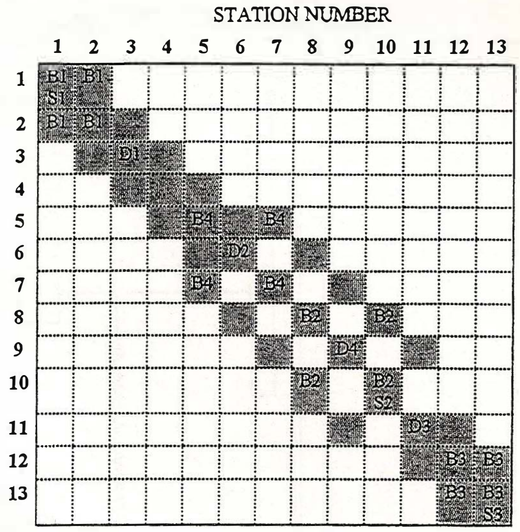

Fig. 5 Proposed system matrices

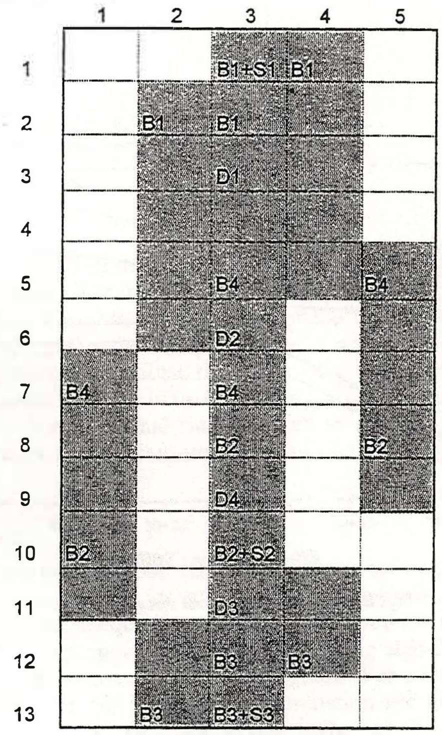

Fig. 6 System matrix in band storage mode

theses are the proposed station numbers. The finite element stations of the model are conventionally numbered consecutively from shafts to supports starting with station 1 at the left end of shaft A to station 6 at the right end of shaft A, and station 7 at the left end of shaft B to station 10 at the right end of shaft B. The support station numbers are assigned from left to right with station numbers 11, 12, and 13. The system equations of motion are assembled by the principle of displacement compatibility and connectivity and are of the form:

$$\mathbf{M}\ddot{\mathbf{q}} + (\mathbf{C} + \mathbf{G})\dot{\mathbf{q}} + \mathbf{K}\mathbf{q} = \mathbf{Q} \tag{10}$$

where the displacement vector is of the form:

$$\mathbf{q} = (\underbrace{\mathbf{q}_1, \ldots, \mathbf{q}_6}_{\text{Shaft A}}, \underbrace{\mathbf{q}_7, \ldots, \mathbf{q}_{10}}_{\text{Shaft B}}, \underbrace{\mathbf{q}_{11}, \mathbf{q}_{12}, \mathbf{q}_{13}}_{\text{Supports}})^T \tag{11}$$

The system matrices are sparse with the forms shown in Fig. 4. With this conventional station numbering scheme, full matrix manipulation algorithms must be employed and they are more time consuming than necessary.

It is proposed that a new station numbering technique be used during the system assembly process. This ordering technique can minimize the matrix bandwidth, the memory storage and can increase computational efficiency. The technique can also be easily programmed to automate the numbering process. This new numbering scheme breaks the barrier between the shaft elements, shafts, and supports. With this new method, the station numbers are assigned values as close as possible to the connecting stations. As illustrated in Fig. 3, the new station

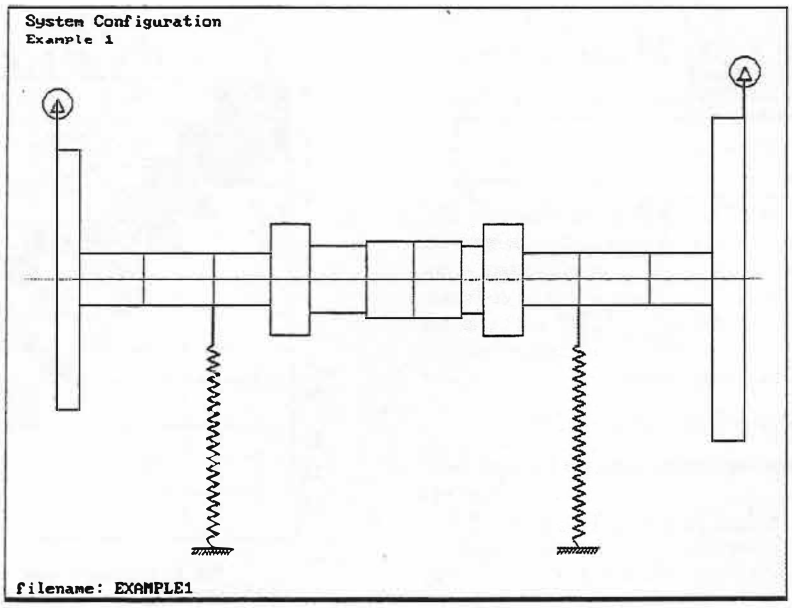

Fig. 7 Schematic plot of industrial compressor

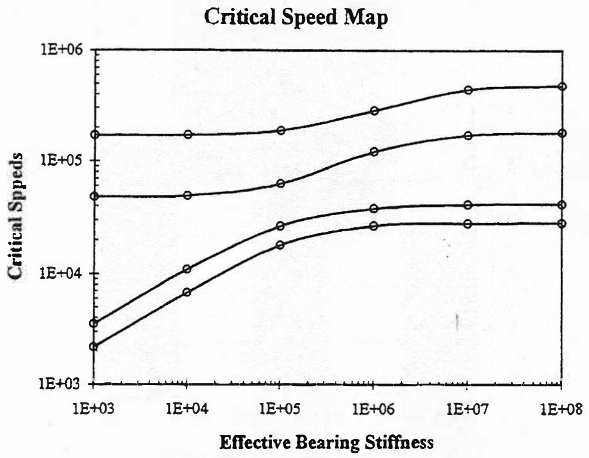

Fig. 8 Undamped critical speed map

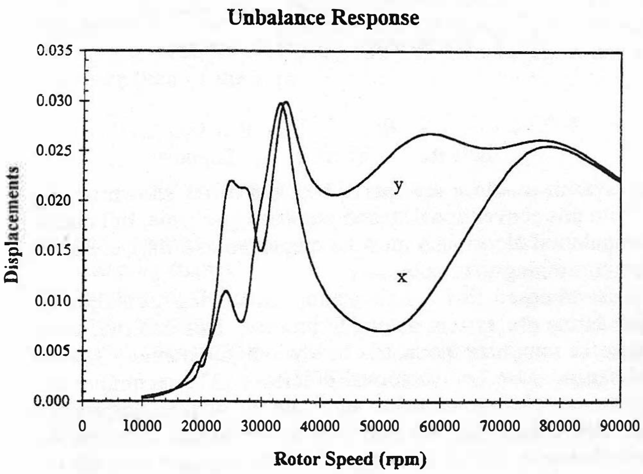

Fig. 9 Steady state unbalance response curves

number 1 is assigned at the first bearing support. Station number 2 is at the connecting bearing station which is also the left end of shaft A. The station numbers increase consecutively to station 5 which is the intershaft bearing station. Following this new numbering strategy, the subsequent station numbers are split between the two shafts as indicated in Fig. 3. The assembled system equations of motion have the same form as given in Eq. (10), however, the bandwidth of the system matrices is significantly reduced, as shown in Fig. 5. To further reduce the computer memory storage requirement, the banded square matrix can be stored in rectangular matrix form with the diagonal terms in the third column, as illustrated in Fig. 6. The benefit of this numbering scheme is clear for systems with multiple shafts and/or flexible supports. With small bandwidth matrices, the memory storage is decreased and the computational efficiency can be improved with the use of modern bandwidth matrix manipulations.

Numerical Examples

Two examples are employed to demonstrate the computational savings of the proposed algorithms. A 90MHz Pentium personal computer with 16MB RAM was used throughout the numerical calculation. The first example is a high speed industrial compressor. The system is a double overhung rotor as shown in Fig. 7. The rotor assembly mass is 2.78 Kg and it is 276 mm long with a journal diameter of 20.8 mm. The rotor is modeled with 14 finite elements (15 stations). The present rotor design speed is 76,500 rpm and a higher speed is expected with further development. Figure 8 shows the undamped critical speed map as a function of effective bearing stiffness. The map was constructed by repeated eigenvalue analysis for various sets of bearing stiffnesses. For six (6) different sets of bearing stiffnesses the total computer run time was 3.4 seconds. The QR algorithm was used as the eigenvalue solver and all the eigenvalues were calculated. About 50 percent of the total run time was on the output of the results and the computational time on the eigenvalue solver was about 1.4 seconds. In general, the critical speed calculation is very fast and the computation time is within seconds. For small-sized bearings, manufacturing tolerances can result in a wide range of bearing clearance and preload (Chen et al., 1994). For some bearing designs, the rotor can actually operate above the third critical speed. The steady

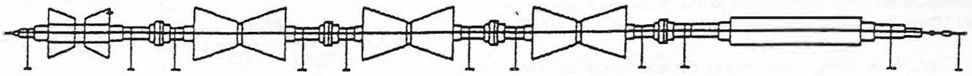

Fig. 10 Schematic plot of turbine-generator system

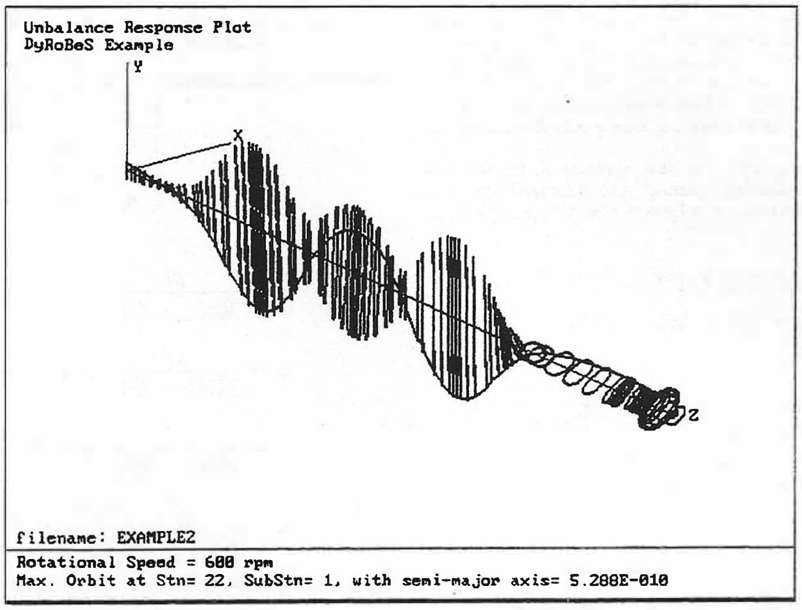

Fig. 11 Unbalance response versus shaft axis

state unbalance response calculation is an important design tool for various bearing designs and configurations. Since the driver of the compressor can be an electrical motor or an engine, the low speed range of the response is also an important factor for determining the warm-up speed. Steady state unbalance response curves for a specific bearing design configuration are shown in Fig. 9. The calculation starts with a speed of 10,000 rpm and ends with a speed of 90,000 rpm using an increment of 500 rpm. The computer run time for the response calculations was about 12 minutes. The computer run time also included the input and output of the results. In a design process, this calculation often needs to be repeated several times and the computation time can be significant. Any savings in the computational effort are clearly beneficial. When complex coordinates and band matrices are employed in this example the computer run time for the same response calculations was reduced to about 8 minutes with the same results.

The second example is a 1150 MW turbine-generator system taken from Gunter et al. (1994). The schematic plot of the rotor system is shown in Fig. 10. The mass of this rotor system is approximate 727,000 Kg and it is 62 m long. The normal operating speed is 1800 rpm. It consists of a high pressure turbine, three low pressure turbines, a generator and an exciter. The rotating assembly is supported by 11 bearings with flexible housings. The rotor system is modeled with 90 elements and 58 disks. Flexible bearing supports are included in the model to accurately predict the dynamic behavior of the system. In the critical speed calculation, a nominal bearing stiffness of 3.5E08 N/m was assumed for all the bearings. The total computer run time for the critical speed calculation was about 8 seconds. The first four calculated critical speeds are 512, 585, 589, and 600 rpm. For this large system, 8 seconds of computer time for critical speed calculations is quite acceptable. However, the computation time for determining the steady state unbalance response over a wide speed range can be very high. The steady state unbalance response at a rotor speed of 600 rpm is shown in Fig. 11. The total computer time for this single speed analysis was approximate 4 minutes and 40 seconds. The computational time from assembling the element equations to solving the system equation was about 52 seconds for the conventional real domain analysis. In the complex domain without station renumbering, the computational time reduced to about 20 seconds. In the complex domain with the global station re-numbering scheme, the computational time reduced to about 2 seconds. This represents a significant improvement in the computational efficiency.

Conclusion

Two coordinate and one station numbering techniques have been summarized in the formulation of the rotordynamic equations. More concise equations are deduced from these proposed procedures. The proposed automatic numbering algorithms can be easily implemented in computer programs. For systems with isotropic supports, the single plane formulation and global station numbering technique can be very effective. For general systems, the complex formulation with the global station numbering technique can significantly reduce the sizes of the matrices and can minimize the bandwidth of the matrices. The proposed procedures provide significant savings in computational efficiency and storage requirements.

References

Childs, D. W., and Graviss, K., 1982, "A Note on Critical-Speed Solutions for Finite-Element-Based Rotor Models," ASME *Journal of Mechanical Design*, Vol. 104, pp. 412–416.

Chen, W. J., Zeidan, F. Y., and Jain, D., 1994, "Design, Analysis, and Testing of High Performance Bearings in a High Speed Integrally Geared Compressor," *Proceedings of 23rd Turbomachinery Symposium*, Texas A&M University, Texas.

Ehrich, F. F., 1992, *Handbook of Rotor-dynamics*, McGraw-Hill, New York, Chapter 2.

Genta, G., 1988, "Whirling of Unsymmetrical Rotors: A Finite Element Approach based on Complex Co-ordinates," *Journal of Sound and Vibration*, Vol. 124, No. 1, pp. 27–53.

Gunter, E. J., Fang, Z., and Henderson, J. R., 1994, "Static and Dynamic Analysis of a 1150 MW Turbine-Generator System—Part I: Static Analysis," *Proceedings of Eighteenth Annual Meeting*, Vibration Institute, Illinois.

Hashish, E., and Sankar, T. S., 1984, "Finite Element and Modal Analyses of Rotor-Bearing Systems Under Stochastic Loading Conditions," Vol. 106, pp. 80–89.

Nelson, H. D., and Chen, W. J., 1993, "Undamped Critical Speeds of Rotor Systems Using Assumed Modes," ASME JOURNAL OF VIBRATION AND ACOUSTICS, Vol. 115, pp. 367–369.

Nelson, H. D., 1985, "Rotor Dynamics Equations in Complex Form," ASME JOURNAL OF VIBRATION, ACOUSTICS, STRESS, AND RELIABILITY IN DESIGN, Vol. 107, pp. 460–461.

Nelson, H. D., 1980, "A Finite Rotating Shaft Element Using Timoshenko Beam Theory," ASME *Journal of Mechanical Design,* Vol. 102, pp. 793–802.

Rouch, K. E., and Kao, J. S., 1979, "A Tapered Beam Finite Element for Rotor Dynamics Analysis," *Journal of Sound and Vibration,* Vol. 66, pp. 119–140.

Ruhl, R. L., and Booker, J. F., 1972, "A Finite Element Model for Distributed Parameter Turborotor Systems," ASME *Journal of Engineering for Industry,* pp. 126–132.

Shiau, T. N., and Hwang, J. L., 1989, "A New Approach to the Dynamic Characteristic of Undamped Rotor-Bearing Systems," ASME JOURNAL OF VIBRATION, ACOUSTICS, STRESS, AND RELIABILITY IN DESIGN, Vol. 111, pp. 379–385.

APPENDIX

Mass/Inertia matrix: $\mathbf{M}_{XZ}^e = \mathbf{M}_T^e + \mathbf{M}_R^e$

Translational mass matrix:

$$\mathbf{M}_T^e = \begin{bmatrix} m_1 & & \text{Sym} & \\ m_2 & m_5 & & \\ m_3 & -m_4 & m_1 & \\ m_4 & m_6 & -m_2 & m_5 \end{bmatrix}$$

where

$$m_1 = \frac{\rho A l}{420(1+\Phi)^2}(156 + 294\cdot\Phi + 140\cdot\Phi^2)$$

$$m_2 = \frac{\rho A l}{420(1+\Phi)^2}(22 + 38.5\cdot\Phi + 17.5\cdot\Phi^2)l$$

$$m_3 = \frac{\rho A l}{420(1+\Phi)^2}(54 + 126\cdot\Phi + 70\cdot\Phi^2)$$

$$m_4 = \frac{\rho A l}{420(1+\Phi)^2}(-13 - 31.5\cdot\Phi - 17.5\cdot\Phi^2)l$$

$$m_5 = \frac{\rho A l}{420(1+\Phi)^2}(4 + 7\cdot\Phi + 3.5\cdot\Phi^2)l^2$$

$$m_6 = \frac{\rho A l}{420(1+\Phi)^2}(-3 - 7\cdot\Phi - 3.5\cdot\Phi^2)l^2$$

Rotatory mass matrix:

$$\mathbf{M}_R^e = \begin{bmatrix} n_1 & & \text{Sym} & \\ n_2 & n_3 & & \\ -n_1 & -n_2 & n_1 & \\ n_2 & n_4 & -n_2 & n_3 \end{bmatrix}$$

where

$$n_1 = \frac{\rho I}{30l(1+\Phi)^2}(36)$$

$$n_2 = \frac{\rho I}{30l(1+\Phi)^2}(3 - 15\cdot\Phi)l$$

$$n_3 = \frac{\rho I}{30l(1+\Phi)^2}(4 + 5\cdot\Phi + 10\cdot\Phi^2)l^2$$

$$n_4 = \frac{\rho I}{30l(1+\Phi)^2}(-1 - 5\cdot\Phi + 5\cdot\Phi^2)l^2$$

Gyroscopic matrix:

$$\mathbf{G}_{XY}^e = -\Omega\cdot 2\mathbf{M}_R^e$$

Stiffness matrix:

$$\mathbf{K}_{XZ}^e = \frac{EI}{l^3(1+\Phi)}\begin{bmatrix} 12 & & \text{Sym} & \\ 6l & (4+\Phi)l^2 & & \\ -12 & -6l & 12 & \\ 6l & (2-\Phi)l^2 & -6l & (4+\Phi)l^2 \end{bmatrix}$$